Journal of Environmental Management 400 (2026) 128767

Contents lists available at ScienceDirect

Journal of Environmental Management

journal homepage: www.elsevier.com/locate/jenvman

Research article

Multi-natural hazard mapping for critical infrastructures in complex territorial contexts: proposal of a novel methodological approach

Maria Castiglione *, Marco Capodici, Santo Fabio Corsino, Alida Cosenza, Michele Torregrossa

Department of Engineering, University of Palermo, Viale delle Scienze, Edificio 8, 90128, Palermo, Italy

ARTICLE INFO

Keywords:
Critical infrastructures
Geographic information systems
Hazard interaction
Multi-hazard assessment
Wastewater treatment plants

ABSTRACT

This study presents a novel methodological approach for multi-hazard assessment (MHA) aimed at evaluating the exposure of critical infrastructures to natural hazards in complex territorial contexts. The proposed approach integrates harmonized hazard maps into a unified geospatial framework including five natural hazards relevant to the Sicilian region: seismic, geomorphological (landslides), hydraulic (floods), volcanic, and tsunami. The assessment relies only on those natural hazards for which authoritative and regionally coherent datasets are available. Other natural and non-natural hazard categories were not considered in this study.

Three different weighting strategies for composing the multi-hazard index (MHI) from the five hazards were tested: i. equal weighting – strategy 1 (S1); ii. presence-based dynamic weighting – strategy 2 (S2); iii. interaction-based dynamic weighting – strategy 3 – (S3), which accounts for hazard interdependencies through adapted interaction matrices.

In this study, wastewater treatment plants (WWTPs) were selected as representative critical infrastructures. The proposed methodological approach was tested in Sicily (Italy), a region where multiple hazards coexist and interact. The results demonstrated that the choice of weighting strategy significantly influenced the spatial distribution and classification of hazard levels. While equal weighting (S1) led to a conservative classification, the presence-based approach (S2) produced a more responsive distribution. The interaction-based approach (S3), which incorporates compound and cascading effects among hazards, emerged as the most balanced, reducing the risk of over- or underestimation of the single hazard. The application of the MHA to Sicily's WWTPs based on S3 revealed that approximately 80 % of facilities are located in areas classified as high or very high hazard. This underscored the critical vulnerability of these infrastructures and highlights the need for hazard-based planning. Future developments should aim to integrate infrastructure-specific vulnerability data to further advance multi-risk modelling frameworks.

1. Introduction

The concept of multi-hazard assessment (MHA) was for the first time introduced in the United Nations' Agenda 21 for sustainable development (UNEP, 2002), as an approach to evaluate multiple hazards that may affect a given area (Wang et al., 2020).

Over time, the concept of MHA has gained increasing relevance. The Johannesburg Plan (United Nations, 2014), described MHA as an "essential element of a safer world in the twenty-first century". In recent years, several attempts of integrating MHA into risk mitigation plans have been performed (De Angeli et al., 2022; Gallina et al., 2016). MHA has a key role in a world with increasing number of natural disasters to prevent their direct (on the critical infrastructures) and indirect (on population and environment health) effects (European Environment Agency, 2010). The European Commission warned that, without significant intervention, the annual damage to European infrastructure could rise dramatically by the end of the century (European Commission, 2018). Therefore, the European Commission has released Directive (EU) 2022/2557. This directive could have important implications for the economic, social, life quality and health of European citizens. Indeed, this Directive requires Member States to identify hazards and develop strategies to increase the resilience of critical infrastructures by January 2026. Therefore, identifying vulnerable areas and critical infrastructures exposed to natural hazards is recognized as a crucial aspect

* Corresponding author.
E-mail address: maria.castiglione01@unipa.it (M. Castiglione).

https://doi.org/10.1016/j.jenvman.2026.128767
Received 11 July 2025; Received in revised form 17 January 2026; Accepted 25 January 2026
Available online 29 January 2026

(Masud and Khan, 2024). Directive (EU) 2022/2557 also provides Member States a unique definition of critical infrastructures often controversial in literature (Smith and Wilson, 2023). Indeed, critical infrastructures are defined as providers of one or more essential services for which any incident would significantly disrupt its ability to provide services or would affect the provision of other essential services (European Parliament Council of the European Union, 2022). Despite the growing attention to multi-hazard assessment, several significant gaps remain in the existing literature (Pourghasemi et al., 2019).

According to the international risk chain framework (UNDRR, 2019), risk arises from the combination of three elements: hazard, defined as a phenomenon with potential harmful effects; exposure, referring to the presence of people and assets in risk-prone areas; and vulnerability, understood as their susceptibility to damage. This study focuses on the hazard–exposure dimension, considered a preliminary yet essential step for critical infrastructure screening, while the explicit integration of vulnerability functions is identified as a future development toward comprehensive risk assessment.

Moreover, most studies focus on individual hazards or address them separately (Novelli et al., 2024; Sun et al., 2021), without considering their dynamic interactions or cascading effects. Even for the cases in which multi-hazard assessments are carried out, a comprehensive understanding of synergistic and sequential hazard relationships is still lacking (Laino and Iglesias, 2024). Therefore, no standardized methodological approach has been still proposed/validated in literature to assign weights to different hazards when generating composite hazard maps. Therefore, the reproducibility and comparability of results across case studies is currently very difficult. This issue is even more pronounced in geographically complex regions, such as islands or coastal and mountainous areas, where the coexistence and interaction of multiple hazards create highly dynamic risk scenarios that are still poorly addressed in current multi-hazard mapping approaches.

Another significant shortcoming in the literature is the limited focus on some critical infrastructure. Their failure or destruction can compromise the delivery of essential services and trigger cascading effects on social well-being (Cantelmi et al., 2021). Some studies in literature have performed attempts on assessing the vulnerability of industrial facilities (Castro Rodriguez et al., 2025; Faggian and Trevisiol, 2024). However, the infrastructures providing relevant services for public health and environmental protection, such as wastewater treatment plants (WWTPs) remains largely underrepresented despite their vulnerability and critical role in environmental resilience. The occurrence of extreme natural events in cause functional losses of WWTPs typically (e.g. reduction of process performances) resulting in the release of untreated or insufficiently treated wastewater into the environment (Kumar et al., 2021; Ranieri et al., 2024). Therefore, integrating such infrastructures into multi-hazard maps becomes crucial to ensure their resilience during their operational lifespan and to prevent public health and environmental protection (Shakou et al., 2019).

In order to overcome the aforementioned gaps in literature, this study proposes a multi-hazard methodological approach to be applied to WWTPs. The proposed methodological approach was developed using officially adopted datasets. Specifically, seismic, geomorphological (landslides), hydraulic (floods), volcanic, tsunami hazards have been considered. Indeed, these hazards represent the dominant natural processes influencing territorial dynamics and potential impacts on critical infrastructures at regional scale. Other natural phenomena, such as storms, heatwaves or droughts, were not included due to the lack of standardized and spatially consistent hazard maps covering the study area. Moreover, other hazard categories (technological, organizational, or social) were not addressed in this study, which aims to develop and test a framework for mapping multiple natural hazards.

The proposed methodology has the key novelty of addressing the challenge of the hazard weighting by exploring alternative approaches to improve the robustness and applicability of multi-hazard mapping. The resulting maps were cross-referenced with the spatial distribution of WWTPs, providing a preliminary evaluation of their hazard's exposure.

2. Materials and methods

2.1. Proposed multi-hazard assessment method

The proposed multi-hazard assessment (MHA) methodology is based on an integrated stepwise procedure developed to ensure consistency among heterogeneous geospatial data. Specifically, the proposed methodology is composed of 8 steps: 1. Identification of the study area; 2. Hazards identification; 3. Thematic maps collection; 4. Harmonization of geospatial data; 5. Grid definition; 6. Individual hazard indicator definition; 7. Multi hazard index definition; 8. Weighting of multi hazard indices.

Fig. S1 summarizes the entire procedural flow proposed.

Each step involves a specific data analysis procedure, which outcomes are essential for implementing the subsequent phase. This stepwise approach leads to the construction of a comprehensive index that accounts for interactions among multiple hazards. In the following section the proposed methodological approach will explained in detail by applying the MHA to WWTPs in Sicily (Italy).

2.1.1. Identification of the study area

The first step of the MHA consisted of identifying the study area and hazard specificities of the geographic area. In this step, it is essential to consider the availability of extensive geospatial data.

In this study, Sicily was selected as a case study area. Indeed, it represents an ideal case study for the development of a multi-hazard assessment due to its exposure to several natural hazard and high territorial vulnerability.

Sicily is the largest island (25,708 km^2) in Italy. Sicily's geology includes mountain chains originated by the collision of the African and Eurasian plates. This interaction generates high seismic and volcanic activity, particularly in the eastern region. Mount Etna, the most active stratovolcano in the world, is an example of this intense geological activity. Moreover, Sicily is exposed to tsunami hazard due to the presence of active coastal and submarine volcanoes, as evidenced by historically documented tsunami events. Furthermore, irregularly distributed faulting layers contribute to widespread landslides. As a result, Sicily is particularly vulnerable to several natural hazards.

2.1.2. Hazards identification

To develop the MHA aimed at evaluating the exposure of WWTPs, an accurate identification of potentially relevant hazards was required. In this step, all the possible natural events that could damage and compromise the structural and functional integrity of such facilities must be considered. Attention was paid towards geophysical and hydrological hazards.

The methodological approach to establish which hazard consider has been firstly based on the map's availability and on the interest towards the WWTP considered as critical infrastructure.

Regarding geophysical hazards, earthquakes, tsunami, landslides, and volcanic eruptions were considered. Specifically, Sicily is a region with high seismicity, so earthquakes could compromise the stability of the civil infrastructures. Landslides, which occur mainly in hilly and mountainous areas, can affect access to the facilities and, in some cases, their structural stability. In addition, the presence of Mount Etna makes volcanic eruptions a hazard that cannot to be underestimated. Indeed, while this phenomenon does not affect all WWTPs, it could have a not negligible impact on those plants located near the volcano. Tsunami was also considered, as coastal wastewater treatment plants may be significantly affected during such events, despite their lower frequency compared to other natural hazards. Regarding the hydrological hazards, flooding was identified as the most relevant. Flash floods triggered by intense rainfall events could cause possible damage to plants and to their operation.

2.1.3. Collection of thematic maps

To evaluate and quantify the main natural hazards in the Sicilian region, a systematic collection of thematic maps was carried out. The thematic maps provided a detailed and georeferenced visualization of the hazards. The hazard maps used in the study were obtained from national and regional authorities, that are officially responsible for hazard assessment and land-use regulation in Italy (National Institute of Geophysics and Volcanology – INGV; Italian National Institute for Environmental Protection and research – ISPRA; Italian Civil Protection Department – DPC and the Sicilian River Basin Authority). These datasets undergo institutional validation and are the reference cartographic sources used for territorial planning, civil protection strategies and infrastructure design. Therefore, in this study the maps were adopted without performing an additional uncertainty analysis. These maps define the hazard level based on objective criteria such as the intensity of the phenomenon and its likelihood of occurrence. Table S1 summarizes the hazard maps used in the study, describing for each type of hazard the data used, the hazard classes identified and the reference sources. The geospatial datasets, consisting of both shapefiles and raster formats, were processed using the Quantum Geographic Information System (QGIS, open-source version 3.32).

2.1.4. Harmonization of geospatial data

A critical challenge in developing a robust multi-hazard assessments lies in the integration of heterogeneous hazard data, particularly when relying on hazard maps characterized by differing classification schemes, spatial resolutions, and methodological frameworks. As a result, the corresponding hazard classes are rarely comparable in either qualitative or quantitative terms, thus hindering the direct overlay of spatial data. Therefore, to ensure comparability between geospatial data from heterogeneous sources, a preliminary harmonization of the datasets must be carried out, both geometrically and in terms of information content.

First, all the hazard maps should be acquired or converted into vector format to ensure consistency and analytical flexibility throughout the multi-hazard assessment. This approach allows for a more precise and scalable representation of geographic features. In this study, all hazard maps were already available in vector format, except for the volcanic map. For this map, a raster-to-vector conversion was performed using a regular grid with the same resolution as the raster. Raster values were assigned to the corresponding vector polygons through centroid-based sampling.

Then, all datasets must be georeferenced by using the same coordinate system, ensuring spatial consistency in the analysis. In this study, the WGS 84/UTM Zone 33N (EPSG:32,633), was chosen due to its accuracy and suitability for large-scale regional studies.

Finally, a normalization of hazard values must be performed to enable comparison between different natural hazards. This process involved adjusting the hazard data from each source to a common scale, accounting for variations in their impact assessments. This step was essential for integrating different hazard maps into a cohesive multi-hazard model. Indeed, it allowed for normalizing different hazard maps while creating a uniform basis for evaluating and comparing the relative intensity and spatial distribution of multiple hazards. In this study, the hazard classes from each map were reclassified into four standardized categories, named H_k (where k = 1, 2, 3, 4). A linear normalization approach was adopted for each hazard map, since, to authors' knowledge, no specific information is available in literature. Thus, a numerical value was assigned to each class: H1 = 0.25, H2 = 0.5, H3 = 0.75, and H4 = 1. The highest value (1) corresponded to the maximum value of the hazard, whereas the lowest (0.25) corresponded to the minimum.

Specifically, the hydraulic and geomorphological hazard maps, initially classified into four qualitative levels, were reclassified with a standardized numerical value: low = 0.25, moderate = 0.5, high = 0.75, very high = 1. A similar approach was applied to seismic the hazard, classified into four zones according to the hazard level: Zone 1 hazard value equal to 1; Zone 2 hazard value equal to 0.75; Zone 3 hazard value equal to 0.5; Zone 4 hazard value equal to 0.25. For tsunami hazard, 0.75 was assigned to orange alert and 1 to red alert, in line with the other hazards classification. The volcanic hazard map was also reclassified. In particular, the continuous probability range (0–0.050) was divided into four equal-width intervals. Standardized numerical values were assigned as follows: $0 < p \leq 0.013$ was assigned a value of 0.25; $0.013 < p \leq 0.025$ of 0.50; $0.025 < p \leq 0.038$ of 0.75; and $p > 0.038$ of 1.

2.1.5. Grid definition

The next step of the methodology involves the creation of a spatial grid to establish a consistent spatial framework for analysis and facilitate the integration of multiple hazard layers across the study area. The resolution of the grid must be chosen to balance spatial resolution and computational efficiency. Indeed, a too fine resolution could result in high computational processing time, whereas a coarse resolution might reduce the accuracy of the results.

In this study, a grid was developed to cover the entire Sicilian territory, with each cell measuring 200 m by 200 m. This grid resolution was selected in accordance with the approach presented by Beltramino et al. (2022), where comparable cell sizes were used for regional-scale analysis of territorial vulnerability and infrastructures exposure. This resolution was selected to provide a sufficient level of spatial detail while ensuring manageable computational demand for the MHA. Each grid cell, named as cell-*i*, represents the spatial unit for the subsequent multi-hazard assessment.

2.1.6. Data integration and calculation of a cell-level hazard indicator

Following the definition of the analysis grid, each hazard map must be intersected with it to align the spatial information. Considering a specific hazard (hazard-j), it is possible that a single grid cell *i* of the spatial grid contains multiple hazard classes, each covering a defined portion of the cell's area.

To cope with this issue, the following approach was proposed in this study. The area of cell *i* corresponding to the hazard class H_k for hazard *j* was named as $A_{i,j,k}$, while the total area of the cell (A_i) was fixed at 40,000 m^2. A relative proportion ($w_{i,j,k}$) was then calculated as the ratio between $A_{i,j,k}$ and A_i (equation (1)). This parameter does not represent an arbitrary weight, but simply the fraction of the cell occupied by each hazard class.

$$w_{i,j,k} = \frac{A_{i,j,k}}{A_i} \quad \text{(eq. 1)}$$

To quantify the contribution of each class to the cell's total hazard level, this proportion ($w_{i,j,k}$) was multiplied by the numerical value assigned to class H_k, derived from the harmonization process

The hazard indicator for hazard *j* in cell *i* ($HI_{i,j}$) was then obtained as the sum of all class contributions (equation (2)):

$$HI_{i,j} = \sum_{k=1}^{n} \left(w_{i,j,k} \cdot H_k \right) \quad \text{(eq. 2)}$$

Where n represents the total number of the hazards categories (n is equal to 4 in this application). The indicator of Equation (2) represents a normalized hazard level for each hazard *j* in each grid cell *i*, allowing for the integration of all the hazards in the MHA. This formulation ensures that the resulting indicator represents a normalized value of hazard intensity for hazard *j* in each grid cell *i*, accounting for both the spatial extent and the severity class of the hazard. This process was repeated for all the type of hazard *j*.

2.1.7. Multi-hazard index definition

After calculating the individual hazard indicators for each type of hazard across the spatial grid, the next step of the methodology involves the definition of a multi-hazard index. This index aims to integrate the

different hazard layers into a single indicator that reflects the cumulative hazard level for each spatial unit.

The multi-hazard index for cell *i* (MHI_i) was computed as a weighted sum of individual hazard indicators obtained in the previous step (equation (3)). The weights λ_j assigned to each hazard *j* was made according three different scenarios described in detail in section 2.1.8.

$$MHI_i = \sum_{j=1}^{N} \left(\lambda_j \cdot HI_{i,j}\right) \quad \text{(eq. 3)}$$

where N represents the total number of hazards taken into account (N is equal to 5 in this study). This composite index provides a single value that expresses the overall level of hazard in each cell, considering the contribution of all the hazards.

Based on the calculated MHI values, a multi-hazard map was generated by classifying the study area into four distinct hazard levels, representing a gradation of potential threats:

- Class 1 (Low Hazard): $0 \leq MHI_i < 0.25$
- Class 2 (Moderate Hazard): $0.25 \leq MHI_i < 0.50$
- Class 3 (High Hazard): $0.50 \leq MHI_i < 0.75$
- Class 4 (Very High Hazard): $MHI_i \geq 0.75$

2.1.8. Strategically weighting the multi-hazard index to account for hazard interactions

In the context of the multi-hazard assessment, a crucial step is to assign weights to the indicators. Indeed, this step could directly influence how the different hazard contributes to the final value of the composite index. Furthermore, not all the hazards have the same likelihood, intensity of impact of the infrastructures. Indeed, some hazards could be more frequent but less destructive, while other could be rare but highly catastrophic.

In this study, three weighting approaches were considered, each representing a different assumption regarding hazard interactions.

2.1.8.1. Scenario 1 – S1: equal weighting approach. As a first scenario, an equal weighting approach was applied. In this case, it was assumed that all hazards contributed equally to the overall hazard. Accordingly, the same weight ($\lambda = 0.20$) was assigned to each hazard considered in the study assuming that all hazard types were present in every grid cell. Therefore, if a hazard was absent from a given cell, it still contributed to the calculation of the multi-hazard index.

2.1.8.2. Scenario 2 – S2: presence-based dynamic weighting. As a second scenario, a dynamic weighting approach was introduced, in which the contribution of each hazard to the multi-hazard index depends on its actual presence within each grid cell. In this case, if a specific hazard was absent from a cell, it was excluded from the calculation. Nevertheless, it was assumed that all present hazards contributed equally to the overall hazard. The dynamic weight $\lambda_{j,i}$ assigned to each hazard (j) and cell (i), is defined accordingly to Equation (4):

$$\lambda_{j,i} = \frac{1}{N_i} \quad \text{(eq. 4)}$$

where N_i is the number of hazards present in cell *i*.

Equation (4) allows that only the hazards occurring within a given cell contributed to the final index, while maintaining the condition that the sum of weights in each cell was equals to 1.

2.1.8.3. Scenario 3 – S3: conditional normalized weighting based on hazard presence. As a third scenario, an alternative method based on the evaluation of natural hazard interactions was adopted. In this context, interaction matrices are key tools for identifying and describing relationships between different natural hazards (Gill and Malamud, 2014; Liu et al., 2016; Van Westen, 2017). As a starting point, the matrices developed by Tilloy et al. (2019) were used. These matrices were derived from an extensive multi-hazard literature review involving 146 references. The original study analysed 14 natural hazards, divided into three main categories (geophysical, atmospheric, and hydrological), and considered 70 references related to interrelationship studies among these hazards. In this study, the original matrices were adapted to reflect the five specific hazards under consideration. This reduction was based on the availability of authoritative, spatially consistent and officially validated datasets at regional scale. The matrix was optimized for the study's context, while preserving the original structure and key interaction types (Fig. S2).

The matrix is structured with primary hazards listed on the left (rows) and secondary hazards along the bottom (columns). Each cell represents the interaction from a primary to a secondary hazard, providing details about how one hazard might influence the occurrence of another. In more detail, four types of interactions are identified: triggering, change conditions, non-sequential and debatable. Moreover, the matrix also indicates the methodological basis of each identified relationship: stochastic (S), empirical (E), mechanistic (M).

Based on this adapted matrix, fixed base weights λ_j' were assigned to each hazard. In particular, the weight of each hazard was determined through a semi-quantitative, expert-informed procedure by considering the number and type of interactions in which it acts as a primary or secondary hazard. Triggering and change-condition relationships were given greater relevance than non-sequential or debatable interactions reflecting their propensity to trigger or be triggered by other hazards. The weights of each hazard have been established on the basis of a trial-and-error approach by assuming that the weight sum is equal to 1. Table 1 shows the assigned weights and the related interpretation.

Subsequently, in order to prevent that these weights do not distort the MHI in cells where only a subset of hazards is present, a normalization factor (x_i) was introduced. The normalization factor x_i is defined as follows (equation (5)):

$$x_i = \frac{1}{\sum_{j \in R} \lambda_j'} \quad \text{(eq. 5)}$$

where R_i, the set of hazards present in cell *i*.

This factor ensured that the sum of weights for the hazards present in a cell equals 1, maintaining consistency across the spatial grid. The final normalized weight $\lambda_{i,j}$ assigned to each hazard j in cell *i* was then calculated as follows (equation (6)):

$$\lambda_{i,j} = \lambda_j' \cdot x_i \quad \text{(eq. 6)}$$

This interaction-based dynamic weighting framework allows the multi-hazard index to better reflect complex hazard interdependencies.

For clarity, the calculation of the S3 weighting scheme can be summarized as follows: 1. Assign a fixed base weight $\left(\lambda_j'\right)$ to each hazard j

Table 1
Weights and description derived from hazard interrelation matrix.

Hazard	λ_j'	Description
Seismic	0.35	Triggers landslides, tsunamis; affects volcanic eruptions and floods. It is the hazard with the most direct connections.
Geomorphological	0.20	It can be triggered by earthquakes and precipitation; can also cause tsunamis. It acts as both primary and secondary hazard.
Hydraulic	0.15	Caused by landslides or earthquakes; limited triggering role but connected to external weather events.
Volcanic	0.20	Related but localized; can cause landslides and earthquakes but is less frequently triggered by other hazards.
Tsunami	0.10	Almost always secondary, triggered by earthquakes or underwater landslides; weak ability to trigger other hazards.

based on the interaction matrix; 2. For each grid cell *i*, identify the subset R_i of hazard present; 3. Compute the normalization factor x_i as the inverse of the sum of base weights of the hazards present in the cell; 4. Derive the normalized weight $\lambda_{i,j}$ for each hazard j in cell *i* by multiplying the base weight λ_j' by the normalization factor x_i. As an illustrative example, if a grid cell contains two hazards with base weights $\lambda_j' = \{0.35, 0.20\}$, the normalization factor is $x_i = 1/(0.35 + 0.20) = 1/0.55$. The corresponding normalized weights are therefore $\lambda_{i,j} = \{0.64, 0.36\}$, ensuring that their sum equals 1. For additional clarity, a methodology flowchart is provided in Fig. S3.

2.2. Assessing WWTP exposure to hazards and MHI methodology validation

To assess the potential exposure of WWTP to natural hazards, the multi-hazard maps resulting from scenarios S1-S3 were overlaid with the spatial distribution of such infrastructures across the study area. This spatial analysis enabled the identification of those treatment facilities located in the areas characterized by different levels of hazard intensity. These records were digitized and georeferenced in a GIS environment. Each WWTP was represented as a point element. This data set was first intersected with the MHI map to assess the overall exposure of wastewater treatment plants.

Furthermore, to validate the multi-hazard methodology, a targeted selection of plants located in different hazard contexts was carried out to validate the consistency and representativeness of the MHI. In more detail, six WWTP located in areas historically affected by documented natural events were selected. These included: Giardini Naxos, Mazara del Vallo, Licata, Misterbianco, Messina and Randazzo. Fig. S4 shows the selected WWTP and the related hazards.

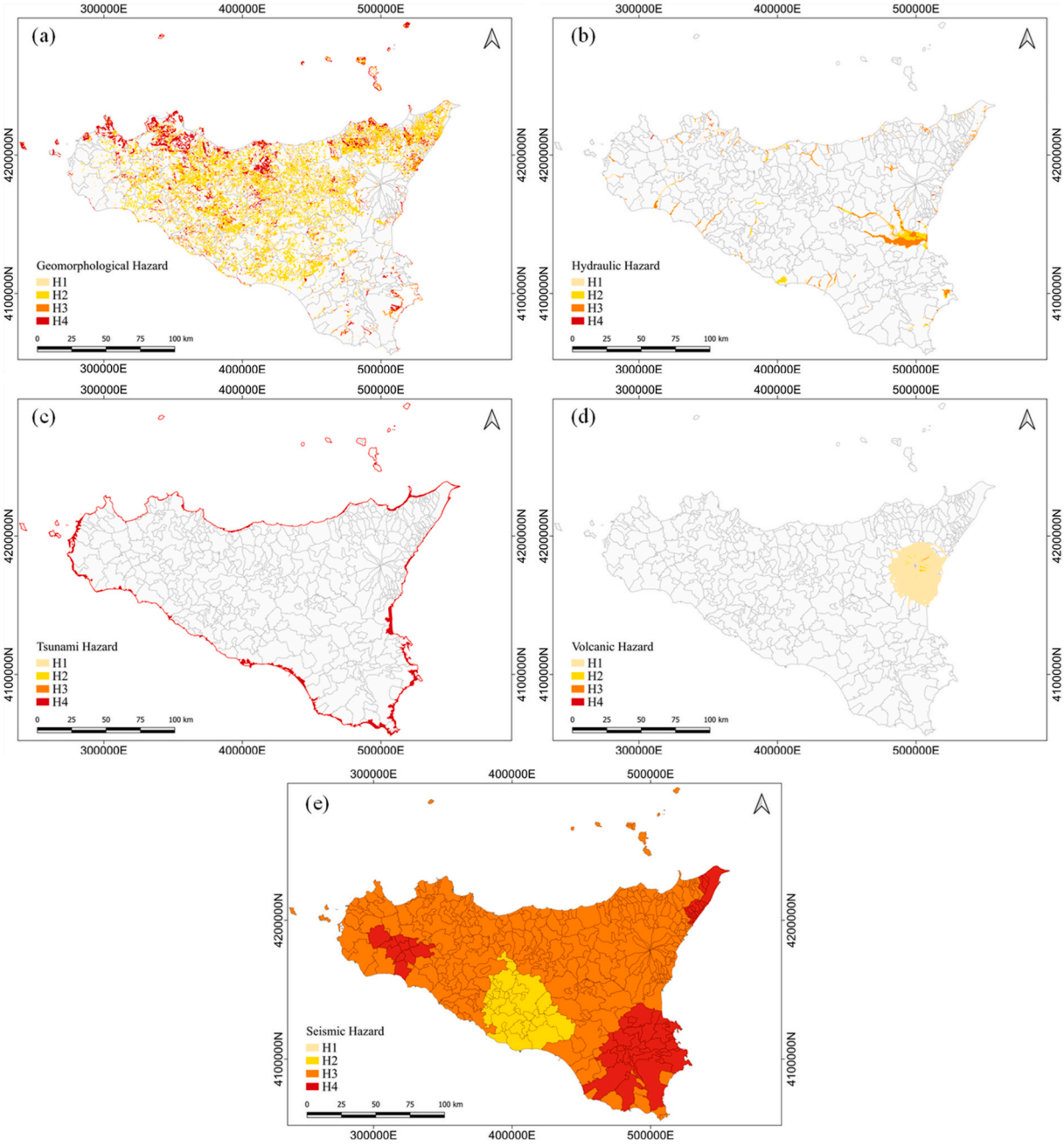

Fig. 1. Hazard indicators for the five hazard types, represented on the analysis grid cells: (a: geomorphological; b: hydraulic; c: tsunami; d: volcanic; e: seismic.

3. Results and discussion

3.1. Harmonization and spatial distribution of single hazard indicators

The initial step of the multi-hazard assessment focused on validating the overlay procedure between the harmonized thematic hazard maps and the analysis grid. This step was crucial to ensure the methodological robustness of the subsequent spatial analysis. Specifically, for each cell of the grid the individual hazard indicators were calculated according to the methodology described in sections 2.1.5 and 2.1.6. These indicators reflected the intensity level of the various hazards considered in this study and served as input for the multi-hazard assessment. The resulting spatial distribution of the indicators is illustrated in Fig. 1.

To verify the consistency of the gridded data with the original hazard datasets, a comparative analysis was conducted. Table 2 presents, for each hazard type, the percentage of the study area falling into each hazard intensity class before and after the harmonization and overlay processes. The comparison demonstrated that the harmonization and overlay procedures have successfully preserved the relative distribution of hazard intensities from the original maps. In fact, considering all the hazards, any statistically significant difference was observed between the area falling into a specific hazard intensity class before and after the harmonization (p-value >0.05). This outcome confirmed the methodological validity of the approach. Indeed, while enabling a uniform representation of diverse hazard layers over a common spatial framework, the process maintained the essential statistical and spatial characteristics of the original data source. Such consistency was a key prerequisite for ensuring that the integrated multi-hazard assessment was both accurate and comparable across different hazards.

To gain a better understanding about the distribution of the various hazard indicators across the region, Table 3 presents a set of descriptive statistics summarizing the spatial characteristics of each hazard type.

The obtained data confirmed that the Sicilian territory is simultaneously affected by multiple natural phenomena, each exhibiting distinct patterns in terms of intensity and spatial variability.

Specifically, the seismic indicator showed a high mean value (0.702) coupled with low variance (0.047) and standard deviation (0.218). This indicated that seismic hazard was not only widespread but also uniformly distributed across a large part of the region. In contrast, both geomorphological and hydraulic indicators presented low mean values (0.133 and 0.119, respectively), while exhibiting high variances (0.358 and 0.493) and standard deviations. These metrics pointed out a highly heterogeneous distribution, with hazard conditions concentrated in specific areas. This is typically the case of regions prone to landslides or flash floods, where localized morphological and hydrological factors play a crucial role.

Table 3
Descriptive statistics of the hazard indicators.

Hazard Indicator	Min	Max	Avg	Var	Std Dev
$HI_{seismic}$	0	1	0.702	0.047	0.218
$HI_{geomorphological}$	0	1	0.133	0.358	0.189
$HI_{hydraulic}$	0	1	0.119	0.493	0.222
$HI_{tsunami}$	0	1	0.538	0.158	0.397
$HI_{volcanic}$	0	1	0.104	0.015	0.123

The tsunami indicator showed a relatively high average value (0.538), coupled with a high standard deviation (0.397), thus revealing considerable spatial variability. This distribution aligned with the nature of this phenomenon, which is limited to coastal zones but can have significant intensity differences depending on local bathymetry and exposure to seismic sources. Similarly, the volcanic hazard indicator had a low mean (0.104) and low variance, thereby reflecting its geographical confinement to a specific volcanic area, around Mount Etna.

Overall, these contrasting statistical metrics highlighted the spatial complexity and diversity of hazard exposure in Sicily. The coexistence of widespread hazards (e.g., seismic and tsunami) with highly localized ones (e.g., volcanic, hydraulic and geomorphological), pointed out the need to overcome a single hazard assessment, while moving toward a multi-hazard approach that considers the different locations and intensities of each hazard.

3.2. Evaluation of multi-hazard index adopting different weighting scenarios

The resulting multi-hazard maps for the three analysed scenarios (S1-S3) are shown in Fig. 2, while Table 4 reports the percentage of the study area assigned to each hazard class in each scenario.

The approach adopted for S1, based on a uniform weighting of all hazard indicators, produced a markedly conservative outcome. Indeed, most of the region (94.7 %) was classified in the lowest multi-hazard class (Class 1), with negligible representation of higher classes. This method considered the presence of all the hazard types in every cell of the analysis grid, regardless of their actual spatial occurrence. Specifically, it assumes that all hazard types were present in every grid cell, which may not reflect reality. As a result, this approach tended to dilute localized high-intensity hazards, leading to an underestimation of the

Table 2
Comparison between original and harmonized hazard maps.

Hazard	Original maps		Maps after harmonization		Absolute difference
	Hazard class	Area coverage (%)	Hazard indicator	Area coverage (%)	
Seismic	Zone 1	17.210	H4	17.209	1.50×10^{-3}
	Zone 2	71.754	H3	71.755	1.40×10^{-3}
	Zone 3	10.608	H2	10.608	2.00×10^{-4}
	Zone 4	0.426	H1	0.426	4.00×10^{-4}
Geomorphological	P1	13.116	H1	13.116	1.00×10^{-4}
	P2	46.318	H2	46.318	3.00×10^{-4}
	P3	9.500	H3	9.500	3.00×10^{-4}
	P4	31.064	H4	31.064	1.00×10^{-4}
Hydraulic	P1	18.243	H1	18.249	5.80×10^{-3}
	P2	29.103	H2	29.106	3.00×10^{-3}
	P3	52.413	H3	52.424	1.07×10^{-2}
	P4	0.239	H4	0.219	1.94×10^{-2}
Tsunami	Orange alert level (Advisory)	21.219	H3	21.208	1.11×10^{-2}
	Red alert level (Watch)	78.780	H4	78.791	1.11×10^{-2}
Volcanic	p = 0–0.013	99.352	H1	99.352	1.00×10^{-4}
	p = 0.013–0.025	0.564	H2	0.564	1.00×10^{-4}
	p = 0.025–0.038	0.062	H3	0.062	5.00×10^{-5}
	p = 0.038–0.05	0.019	H4	0.019	4.00×10^{-5}

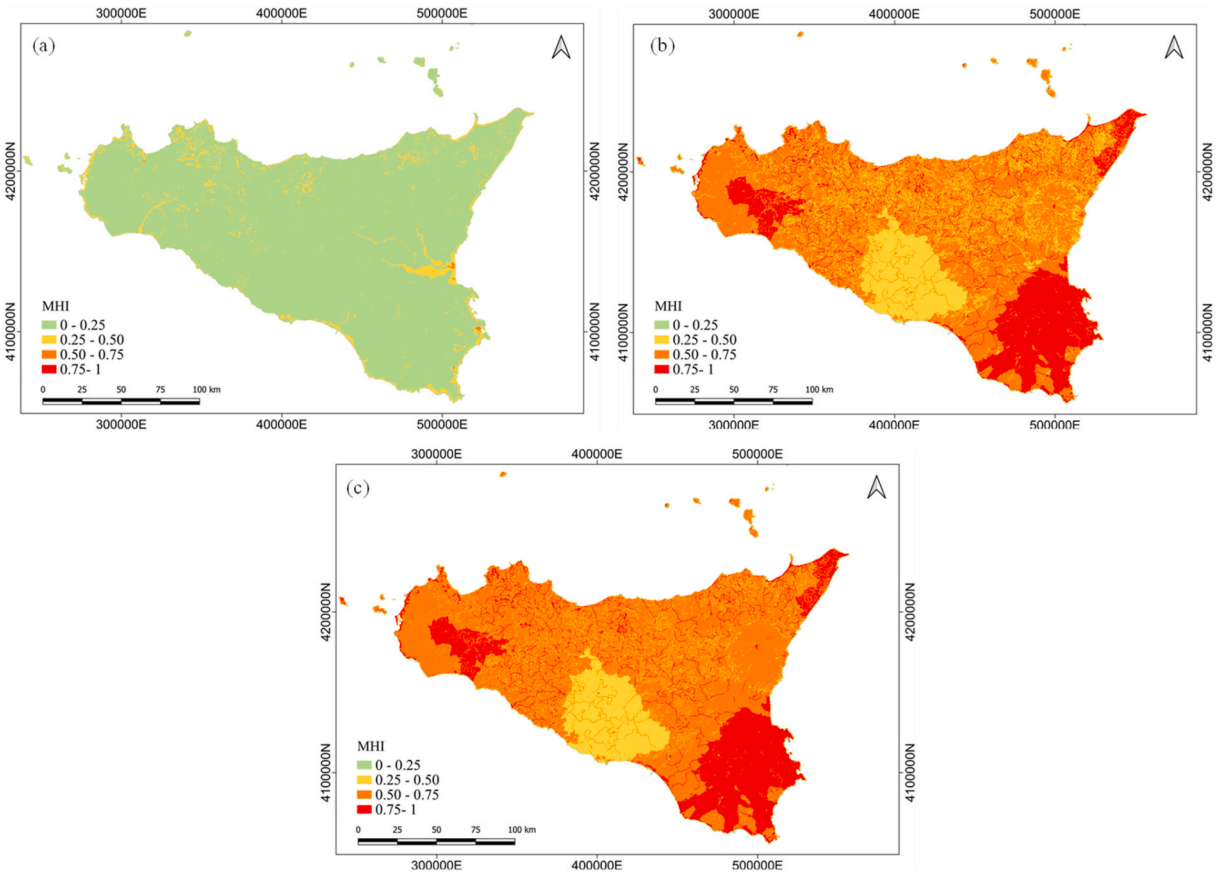

Fig. 2. Multi hazard maps for the three scenarios: (a: S1; b: S2; c: S3).

Table 4
Surface percentages for each hazard class in S1, S2, and S3.

MHI class	S1 (% of area)	S2 (% of area)	S3 (% of area)
Class 1	94.70	0.94	0.92
Class 2	5.22	24.02	16.22
Class 3	0.08	52.29	59.74
Class 4	0	22.75	23.11

actual multi-hazard exposure in areas affected by only one or two significant hazards. Despite this approach has the advantage of being computationally simple and useful for preliminary or comparative purposes, it failed to adequately reflect the spatial heterogeneity and uneven distribution of hazard intensities across the territory.

Scenario S2 introduced a differentiated weighting strategy, whereby hazard indicators were weighted based on their actual presence in each grid cell. This approach resulted in a noticeable different hazard classification. Indeed, only 0.94 % of the area was classified in Class 1, while Classes 3 and 4 (high and very high hazard) covered about 75 % of the study area. This scenario (S2) enhanced the model's capacity to be more locally responsive, providing a more realistic reflection of spatial variations in hazard distribution. More precisely, hazard zones previously underrepresented, such as those affected by tsunami or volcanic activity, became more visible in the classification. However, despite this improvement, S2 still considered hazard indicators as independent, not involving possible interactions or cascading effects among them. In such a way, secondary hazards, which occurrence is strictly related to the activation of other hazards (e.g., tsunami is a secondary hazard respect to seismic) had the same impact of primary ones on the multi hazard indicators. This could potentially lead to an overestimation of multi-hazard exposure in areas where the impact of such secondary hazards is conditional or less probable. This lack of hazard interrelation modelling can distort the risk classification and reduce the interpretive accuracy of the resulting maps.

This limitation was overcome by the approach adopted in S3. Specifically, the assessment was further refined by including the interrelationships between hazards into the weighting strategy. This approach considered that some hazards were not independent but might be causally linked (e.g., tsunami hazard as a secondary effect of seismic activity) and adjusted the contribution of each indicator accordingly. Therefore, a more selective and spatially coherent hazard classification was obtained. Overall, classes 3 and 4 together represent over 82 % of the territory, with a notable dominance of Class 3. This configuration reflects a more integrated and precautionary view of hazard exposure, where multi-hazard interactions amplify the significance of certain areas.

The comparison between S2 and S3 showed that most of the differences were found in MHI Classes 2 and 3, while Classes 1 and 4 remained mostly unchanged. This was mainly due to how secondary hazards were treated. Indeed, in S2, all hazards present in a cell of the grid were considered separately with the same weight, even if some of them only occur when triggered by another hazard. For example, tsunami hazards were considered as independent to the occurrence of seismic events. This can lead to higher hazard values. While, considering the interdependence among hazards as in the S3, secondary hazards were weighted less when their occurrence was conditional, thereby reducing their influence in cells where the triggering primary hazard was absent or of low intensity. Consequently, some areas that were previously assigned to MHI-Class 2 in S2 might shift to MHI-Class 3 in S3 due to the relative increase in the contribution of primary hazards or may be reclassified downward if the overall hazard intensity was rebalanced. As a result, MHI-class 1 and class 4 remained largely unaffected as in such areas

conditions of very low or very high hazard were already clear so that changes in the weighting methods had little effect on these two extreme classes. In contrast, the main differences among the scenarios emerged in the intermediate classes (Class 2 and Class 3), where the weights assigned to hazards and the way the hazards could interact can significantly influence the final classification.

3.3. Assessing WWTPs exposure to multi-hazard conditions

Following the development of the MHI map, the analysis was extended to evaluate the spatial relationship between the distribution of WWTPs and the multi-hazard classification. The resulting spatial patterns are illustrated in Fig. 3.

The spatial analysis showed a marked concentration of WWTPs along coastal areas, particularly in the northwestern sector, the northeast, and along the eastern coast (Fig. 3a). This spatial pattern reflected the location of major urban centres along the coast, which naturally determined the site of wastewater treatment facilities near these population hubs. Additionally, several WWTPs are distributed along the slopes of Mount Etna, a densely populated and industrialized area despite its high exposure to volcanic and seismic hazards. Although the central and southern inland areas of Sicily are generally less urbanized, a non-negligible number of WWTPs are present, confirming the wide coverage of this type of infrastructure across the entire region.

By intersecting the spatial distribution of WWTPs with the MHI, it was possible to assess their exposure to multiple hazard types. The obtained results showed that a substantial number of WWTPs fall within the higher risk categories of the MHI (Fig. 3b). Specifically, 58.15 % of plants resulted located in Class 3 (high hazard) areas and 21.89 % in Class 4 (very high hazard) zones. Therefore, nearly 80 % of the regional WWTP infrastructures resulted potentially exposed to multi-hazard conditions. In contrast, less than 20 % of the WWTP facilities fall in the medium-low hazard class (Class 2) and less than 2 % in the lowest hazard class (Class 1). This result reflected the fact that most of the WWTP are in coastal and urban areas where multiple natural hazards overlapped, leading to higher hazard classifications. Moreover, the coexistence of several simultaneous hazards in the same area contributed to increase the overall exposure of WWTP infrastructures.

3.4. Validation of the multi-hazard approach through selected WWTPs

The validation of the proposed multi-hazard assessment is intended as a consistency-based evaluation rather than as a quantitative validation against observed damage or operational failure data. Accordingly, the validation focuses on assessing the coherence between the spatial distribution of the MHI index and documented hazard occurrences affecting selected WWTPs. To evaluate the robustness and reliability of the proposed multi-hazard methodology, the estimated MHI values obtained in the three study scenarios were compared with documented hazard contexts of a representative selection of WWTPs, based on historical information on natural events that have affected the corresponding territorial areas. (Fig. S4). This comparative analysis aimed to verify the consistency between the model's hazard classifications and the empirical evidence available for each site. Table 5 reports a comparison for each selected WWTP between the MHI obtained by applying the three weighting scenarios and the single HI for each hazard.

The MHI values obtained from the three scenarios showed varying degrees of consistency with the documented hazard conditions at the selected WWTP sites. For instance, the WWTPs in Messina and Giardini Naxos, known for being affected by high-severity seismic and tsunami events in the past, were consistently classified in the highest hazard classes in scenarios 2 and 3. Indeed, their MHI values reach or exceed 0.9 in S3, highlighting their critical exposure in contexts of hazard interaction. This result was mainly due to the strong seismic hazard, which represents a dominant primary hazard in this area. Additionally, there is a significant tsunami risk (HI = 0.572), which is directly dependent on seismic events. This combination of a high-intensity primary hazard (earthquake) and a secondary hazard represents a synergistic interaction between hazards, leading to particularly elevated MHI values, especially in S3, where such interactions were explicitly considered.

Similarly, Mazara del Vallo and Licata' WWTPs, which have experienced moderate-to-high natural events, were classified in the "moderate" to "high" range across all scenarios, reflecting a balanced hazard profile. In contrast to what previously observed for the cases of Messina and Giardini Naxos, in this case although the tsunami hazard index was high (0.64 and 0.97, respectively), the resulting MHI remained at moderate or moderately high levels. This was likely because the seismic hazard in these areas is lower (HI = 0.75 for Mazara del Vallo, 0.50 for Licata), which reduced the likelihood of tsunami activation, since it is a secondary hazard dependent on a seismic trigger. Moreover, other hazards (e.g., hydraulic risk) do not reach critical levels that would otherwise raise the MHI further.

Particularly interesting were the cases of Misterbianco and Randazzo, where less frequent but locally relevant hazards, such as landslides and volcanic activity, are present. In these cases, the progressive increase in MHI from Scenario 1 to Scenario 3 demonstrated the method's ability when hazard interrelationships were considered. For example, the Randazzo' WWTP, situated in an area exposed to both volcanic and seismic hazards, was classified as "Low" in Scenario 1 because only the most dominant single hazard was considered. However, in Scenario 3, which accounted for the combined effect of multiple interacting hazards, the classification rose to "High." This shift better

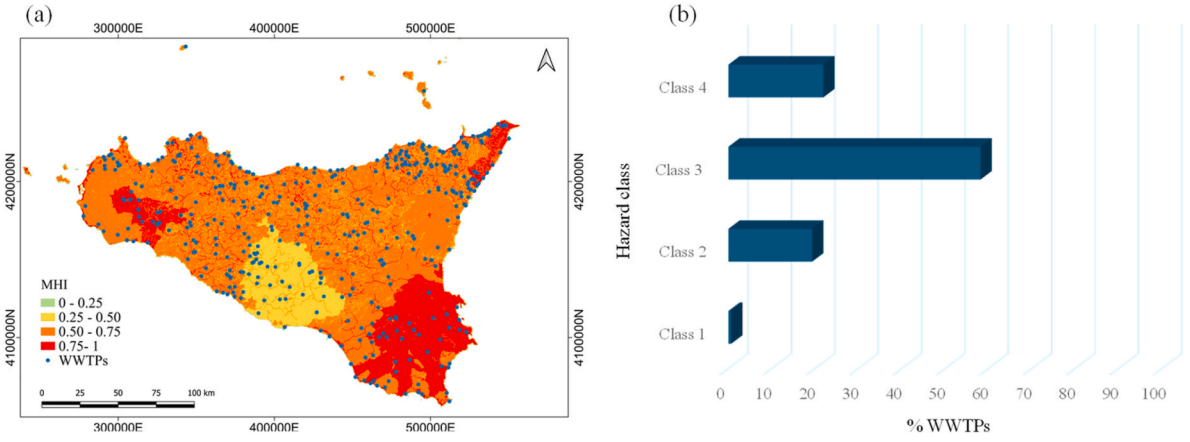

Fig. 3. Spatial distribution of WWTPs in Scenario 3 with classification based on the MHI: (a) map showing plant locations; (b) percentage of plants in each hazard class.

Table 5
Multi-hazard classification of selected WWTPs based on calculated HI and MHI values across three scenarios.

WWTP	Hazards	HI	MHI S1	MHI S2	MHI S3
Giardini Naxos	Seismic	0.75	0.448	0.746	0.726
	Hydraulic	0.49			
	Tsunami	1			
	MHI Class →		Moderate	Very high	Very high
Mazara del Vallo	Seismic	0.75	0.386	0.644	0.679
	Hydraulic	0.54			
	Tsunami	0.64			
	MHI Class →		Moderate	High	High
Licata	Seismic	0.5	0.296	0.493	0.455
	Hydraulic	0.06			
	Tsunami	0.97			
	MHI Class →		Moderate	Moderate	Moderate
Misterbianco	Seismic	0.75	0.195	0.488	0.559
	Geomorphological	0.23			
	MHI Class →		Low	Moderate	High
Messina	Seismic	1	0.315	0.786	0.905
	Tsunami	0.5725			
	MHI Class →		Moderate	Very high	Very high
Randazzo	Volcanic	0.25	0.20	0.50	0.568
	Seismic	0.75			
	MHI Class →		Low	Moderate	High

reflected the actual systemic vulnerability of the area, where the coexistence and potential interaction of different natural hazards significantly increased the overall exposure.

Overall, the comparative analysis of the three scenarios highlighted important differences in the way multi-hazard exposure is represented. The approach adopted in Scenario 1 caused an oversimplification of the overall multi-hazard, failing to account for the combined effect of multiple hazards. This leads to lower or moderate classifications, even in areas known to be exposed to significant multi-hazard threats. In contrast, Scenario 2 resulted in an overestimation of the MHI especially in areas where secondary hazards (e.g., tsunami) are unlikely to occur independently of a primary trigger. Scenario 3, instead, allowed to avoid both underestimation and overestimation, offering a more realistic assessment. Indeed, in areas where strong earthquakes and tsunami events have occurred (e.g., Messina and Giardini Naxos), Scenario 3 assigned very high MHI values, correctly reflecting the severity and nature of past events. Conversely, in Mazara del Vallo and Licata, despite high tsunami HI values, Scenario 3 provided moderate-to-high MHI scores, accurately accounting for the moderate seismic hazard and the conditional nature of tsunami events. The comparison between calculated MHI values and historical evidence highlights some apparent discrepancies between exposure-based indicators and documented events. In particular, some WWTPs classified in moderate-high MHI classes under Scenario 3 (e.g., Mazara del Vallo and Licata) have not experienced documented extreme events, reflecting elevated exposure. Conversely, cases such as Randazzo show that simplified approaches based on dominant single hazards may underestimate exposure, while the interaction-based approach (Scenario 3) provides a more comprehensive representation of potential multi-hazard conditions.

Therefore, this approach can be considered a robust and reliable tool for supporting hazard-based decisions, especially in regions where multiple natural hazards coexist and may interact in compound or cascading ways.

3.5. Implications, limitations, and future perspectives

This study contributes to improve the understanding and management of natural hazards in complex territorial context such as Sicily, where multiple threats often coexist and interact. Despite being tested in Sicily, the proposed methodology is quite flexible and transferable to other territories with different hazard settings and data conditions. Overall, the proposed approach provided a tool to support environmental planning and risk governance to cope the prescriptions of Directive (EU) 2022/2557. From a practical standpoint, the results could have direct implications for land-use management, civil protection, and infrastructure resilience. Specifically, based on the obtained results authorities could prioritize interventions aimed at enhancing operational continuity during extreme events.

The proposed multi-hazard framework is explicitly designed to operate on officially validated hazard maps commonly adopted for spatial planning and decision support purposes. Consequently, the resulting multi-hazard index reflects the assumptions embedded in these authoritative datasets. Within the multi-hazard multi-risk literature, this study is intentionally positioned as a multi-hazard exposure assessment rather than as a comprehensive multi-risk model. In this perspective, the proposed framework focuses on hazard exposure and does not explicitly consider the structural and functional vulnerability of the individual WWTPs. Therefore, to move towards a more integrated risk assessment and management framework, future research should focus on including site-specific vulnerability data (e.g., plant potential, critical components, plant design), in order to develop a multi-risk index that reflects more accurately the potential service disruption. Moreover, the hazard harmonization procedure adopted in this study is based on a linear discretization approach. Although this choice ensures consistency across different hazard types, future studies should explore alternative normalization strategies. Additionally, the current hazard maps are static. Indeed, these maps show the situation at a precise time and do not reflect how hazards may change in the future. Therefore, they do not capture long-term trends, such as those related to climate change. Predictive models that simulate how hazards might evolve over time are advisable for the future. The results of these models could guide long-term adaptation strategies. A further aspect to be considered relates to the assignment of weights in Scenario 3, which in the present study constitutes a preliminary approach. Consequently, this methodological choice should be explored in future research. Lastly, an important future direction is the integration of more specific uncertainty and sensitivity analyses, aimed at evaluating the influence of input assumptions.

4. Conclusions

In this study, a comprehensive methodology for multi-hazard assessment specifically aimed at evaluating the exposure of WWTPs to multiple natural hazards was proposed. The methodology was validated by using a complex territorial context like the Sicilian region in which

many hazard coexist and interact. Three scenarios (S1-S3) testing different weighting approaches were implemented. The interaction-based dynamic weighting (S3) proved to be the most effective in capturing both spatial variability and the cascading nature of natural hazards. Indeed, S3 was most effective in accounting the hazard interdependencies, offering a more realistic and spatially coherent assessment of multi-hazard assessment. The application of the multi hazard assessment to the Sicilian network of WWTPs revealed that approximately 80 % of these facilities are located in areas classified as high or very high hazard zones. Thus, underlying the need of tailoring risk mitigation strategies and resilient infrastructure planning. However, the current model does not incorporate infrastructure-specific vulnerability factors. Therefore, future research should aim to integrate these elements into a multi-risk framework that combines hazard, exposure and vulnerability characteristics.

CRediT authorship contribution statement

Maria Castiglione: Writing – original draft, Methodology, Investigation, Data curation, Conceptualization. **Marco Capodici:** Writing – review & editing, Validation, Methodology. **Santo Fabio Corsino:** Writing – review & editing, Writing – original draft, Methodology, Data curation, Conceptualization. **Alida Cosenza:** Writing – review & editing, Validation, Methodology. **Michele Torregrossa:** Writing – review & editing, Validation, Supervision, Methodology, Conceptualization.

Declaration of competing interest

The authors declare that they have no known competing financial interests or personal relationships that could have appeared to influence the work reported in this paper.

Acknowledgments

This study was funded by the European Union - Next Generation EU, Mission 4 Component 2 RETURN Project, CUP B73C22001220006, PE0000005. Specifically, the research activity falls within the Spoke TS2-Multi Risk Resilience of Critical Infrastructures. WP 3 - Dynamic mapping of natural and climatic hazards over the infrastructure systems. T 3.2 – Robust hazard mapping over point critical infrastructures. Sub Task 3.2.2. Natural Hazards classification maps of point-like infrastructures of national relevance.

Appendix A. Supplementary data

Supplementary data to this article can be found online at https://doi.org/10.1016/j.jenvman.2026.128767.

Data availability

Data will be made available on request.

References

Beltramino, S., Scalas, M., Castro Rodríguez, D.J., Brunetta, G., Pellerey, F., Demichela, M., Voghera, A., Longhi, A., Mutani, G., Caldarice, O., Miraglia, G., Lenticchia, E., La Riccia, L., 2022. Assessing territorial vulnerability. Testing a multidisciplinary tool in Moncalieri, Italy. TeMA – J. Land Use, Mobil. Environ. 15 (3), 355–375. https://doi.org/10.6092/1970-9870/9069.

Cantelmi, R., Di Gravio, G., Patriarca, R., 2021. Reviewing qualitative research approaches in the context of critical infrastructure resilience. Environ. Syst. Decis. 41, 341–376. https://doi.org/10.1007/s10669-020-09795-8.

Castro Rodriguez, D.J., Barresi, A.A., Demichela, M., 2025. Multi-scale characterization of industrial infrastructure vulnerability to multiple hazards in their territories. J. Saf. Sci. Resil. 6 (2), 297–315. https://doi.org/10.1016/j.jnlssr.2024.11.004.

De Angeli, S., Malamud, B.D., Rossi, L., Taylor, F.E., Trasforini, E., Rudari, R., 2022. A multi-hazard framework for spatial-temporal impact analysis. Int. J. Disaster Risk Reduct. 73, 102829. https://doi.org/10.1016/j.ijdrr.2022.102829.

European Commission, 2018. Report from the Commission to the European Parliament and the Council - on the Implementation of the EU Strategy on Adaptation to Climate Change. COM(2018) 738 Final 19.

European Environment Agency, 2010. Mapping the impacts of natural hazards and technological accidents in Europe. Eur. Environ. Agen. https://doi.org/10.2800/62638.

European Parliament Council of the European Union, 2022. Directive (EU) 2022/2557 of the European Parliament and of the Council of 14 December 2022 on the resilience of critical entities and repealing Council Directive 2008/114/EC. Off. J. Eur. Union L 333, 164–198, 2022, 164–198.

Faggian, P., Trevisiol, A., 2024. Climate extreme scenarios affecting the Italian energy system with a multi-hazard approach. Bull. Atmos. Sci. Technol. 5, 1–22. https://doi.org/10.1007/s42865-024-00067-w.

Gallina, V., Torresan, S., Critto, A., Sperotto, A., Glade, T., Marcomini, A., 2016. A review of multi-risk methodologies for natural hazards: consequences and challenges for a climate change impact assessment. J. Environ. Manag. 168, 123–132. https://doi.org/10.1016/j.jenvman.2015.11.011.

Gill, J.C., Malamud, B.D., 2014. Reviewing and visualizing the interactions of natural hazards. Rev. Geophys. 680–722. https://doi.org/10.1002/2013RG000445.

Kumar, N., Poonia, V., Gupta, B.B., Goyal, M.K., 2021. A novel framework for risk assessment and resilience of critical infrastructure towards climate change. Technol. Forecast. Soc. Change 165, 120532. https://doi.org/10.1016/j.techfore.2020.120532.

Laino, E., Iglesias, G., 2024. Multi-hazard assessment of climate-related hazards for European coastal cities. J. Environ. Manag. 357, 120787. https://doi.org/10.1016/j.jenvman.2024.120787.

Liu, B., Siu, Y.L., Mitchell, G., 2016. Hazard interaction analysis for multi-hazard risk assessment: a systematic classification based on hazard-forming environment. Nat. Hazards Earth Syst. Sci. 16, 629–642. https://doi.org/10.5194/nhess-16-629-2016.

Masud, S., Khan, A., 2024. Policy implementation barriers in climate change adaptation: the case of Pakistan. Environ. Policy Gov. 34, 42–52. https://doi.org/10.1002/eet.2054.

Novelli, F., Pesce, F., Bubbico, R., 2024. Seismic risk in the chemical process industry: a semi-quantitative methodology for critical equipment identification. J. Loss Prev. Process. Ind. 88, 105252. https://doi.org/10.1016/j.jlp.2024.105252.

Pourghasemi, H.R., Gayen, A., Panahi, M., Rezaie, F., Blaschke, T., 2019. Multi-hazard probability assessment and mapping in Iran. Sci. Total Environ. 692, 556–571. https://doi.org/10.1016/j.scitotenv.2019.07.203.

Ranieri, E., D'Onghia, G., Lopopolo, L., Gikas, P., Ranieri, F., Gika, E., Spagnolo, V., Herrera, J.A., Ranieri, A.C., 2024. Influence of climate change on wastewater treatment plants performances and energy costs in Apulia, south Italy. Chemosphere 350, 141087. https://doi.org/10.1016/j.chemosphere.2023.141087.

Shakou, L.M., Wybo, J.L., Reniers, G., Boustras, G., 2019. Developing an innovative framework for enhancing the resilience of critical infrastructure to climate change. Saf. Sci. 118, 364–378. https://doi.org/10.1016/j.ssci.2019.05.019.

Smith, K., Wilson, I.D., 2023. Critical infrastructures: a comparison of definitions. Int. J. Crit. Infrastructures 19, 323–339. https://doi.org/10.1504/IJCIS.2023.132213.

Sun, Q., Nazari, R., Karimi, M., Fahad, M.G.R., Peters, R.W., 2021. Comprehensive flood risk assessment for wastewater treatment plants under extreme storm events: a case study for New York city, United States. Appl. Sci. 11. https://doi.org/10.3390/app11156694.

Tilloy, A., Malamud, B.D., Winter, H., Joly-Laugel, A., 2019. A review of quantification methodologies for multi-hazard interrelationships. Earth Sci. Rev. 196, 102881. https://doi.org/10.1016/j.earscirev.2019.102881.

UNEP, 2002. Report of the World Summit on Sustainable Development, 26 Augustus - 4 September 2002.

UNDRR, 2019. Global Assessment Report on Disaster Risk Reduction. United Nations Office for Disaster Risk Reduction, Geneva, Switzerland. https://www.undrr.org/gar2019.

United Nations, 2014. United Nations conference on environment and development. Encycl. Geogr. https://doi.org/10.4135/9781412939591.n1173.

Van Westen, C., 2017. Multo-hazard risk assessment and decision making. In: Environmental Hazards Methodologies for Risk Assessment and Management, pp. 31–94. https://doi.org/10.2166/9781780407135.

Wang, J., He, Z., Weng, W., 2020. A review of the research into the relations between hazards in multi-hazard risk analysis. Nat. Hazards 104, 2003–2026. https://doi.org/10.1007/s11069-020-04259-3.